Fracture-Controlled Paleo-Fluid Flow in Candor Chasma, Mars

Chris H. Okubo, *et al.*

Science **315**, 983 (2007);
DOI: 10.1126/science.1136855

Science (print ISSN 0036-8075; online ISSN 1095-9203) is published weekly, except the last week in December, by the American Association for the Advancement of Science, 1200 New York Avenue NW, Washington, DC 20005.

Successive infusions of hybrid melt into the nascent pluton would therefore precipitate zircons with higher δ^{18}O and lower εHf values, as recorded by the zircon isotope arrays. Zircons with disparate isotope signatures are juxtaposed by mingling and crystal exchange between melt batches during pluton assembly and intrareservoir crystal-liquid sorting (*27*, *31*). Mixing with the recharge melt would also drive the resident magma and its crystallizing zircon cargo toward higher δ^{18}O and lower εHf values, explaining the intrazircon isotope zoning. Isotopic reversals in some zircons and basalt injection in the Why Worry plutons suggest that this evolution was punctuated by juvenile magma replenishments.

The refined view of granite genesis captured by the zircon isotope data compels a reappraisal of the I-S type concept and its implications for crustal evolution. In revealing the reworking of supracrustal material by juvenile magmas, our study suggests that I-type magmatism critically involves continental growth, this being camouflaged to some extent by the non–mantle-like isotope ratios of the bulk rocks. The overall proportion of new material added by the Lachlan I-type suites was near 85% for Cobargo, 70% for Jindabyne, and 50% for Why Worry. These estimates imply that Phanerozoic crust generation rates may have been higher than hitherto appreciated from studies of plutonic terranes (*6*, *32*), modifying global continental growth curves through time.

References and Notes

1. I. H. Campbell, S. R. Taylor, *Geophys. Res. Lett.* **10**, 1061 (1983).
2. D. J. DePaolo, *Science* **209**, 684 (1980).
3. P. J. Hamilton, R. K. O'Nions, R. J. Pankhurst, *Nature* **287**, 279 (1980).
4. M. T. McCulloch, B. W. Chappell, *Earth Planet. Sci. Lett.* **58**, 51 (1982).
5. C. M. Gray, *Earth Planet. Sci. Lett.* **70**, 47 (1984).
6. B.-M. Jahn, F. Wu, B. Chen, *Trans. R. Soc. Edinb. Earth Sci.* **91**, 181 (2001).
7. A. J. R. White, B. W. Chappell, *Tectonophysics* **43**, 7 (1977).
8. S. M. Keay, W. J. Collins, M. T. McCulloch, *Geology* **25**, 307 (1997).
9. B. W. Chappell, *J. Petrol.* **37**, 449 (1996).
10. J. P. Davidson, F. J. T. Tepley, *Science* **275**, 826 (1997).
11. T. E. Waight, R. Maas, I. A. Nicholls, *Contrib. Miner. Petrol.* **139**, 227 (2000).
12. J. R. Vazquez, M. R. Reid, *Science* **305**, 991 (2004).
13. W. L. Griffin *et al.*, *Lithos* **61**, 237 (2002).
14. J. W. Valley *et al.*, *Contrib. Mineral. Petrol.* **150**, 561 (2005).
15. A. I. S. Kemp, M. J. Whitehouse, C. J. Hawkesworth, M. K. Alarcon, *Contrib. Mineral. Petrol.* **150**, 230 (2005).
16. R. Hine, I. S. Williams, B. W. Chappell, A. J. R. White, *J. Geol. Soc. Aust.* **25**, 219 (1978).
17. The δ^{18}O notation signifies deviation of the measured ^{18}O/^{16}O value from Vienna standard mean ocean water in parts per thousand.
18. Materials and methods are available as supporting material on *Science* Online.
19. W. H. Peck, J. W. Valley, C. M. Graham, *Am. Mineral.* **88**, 1003 (2003).
20. J. M. Eiler, *Rev. Mineral.* **43**, 319 (2001).
21. The epsilon notation signifies deviation of the isotope ratio (^{176}Hf/^{177}Hf and ^{143}Nd/^{144}Nd) from a chondritic reference in parts per ten thousand.
22. J. S. Lackey, J. W. Valley, J. B. Saleeby, *Earth Planet. Sci. Let* **235**, 315 (2005).
23. D. J. DePaolo, *Earth Planet. Sci. Lett.* **53**, 189 (1981).
24. J. W. Valley, A. J. Cavosie, B. Fu, W. H. Peck, S. A. Wilde, *Science* **312**, 1139a (2006).
25. A. B. Thompson, L. Matile, P. Ulmer, *J. Petrol.* **43**, 403 (2002).
26. C. J. Hawkesworth, S. Turner, R. George, G. Zellmer, *Earth Planet. Sci. Let* **218**, 1 (2004).
27. R. A. Wiebe, W. J. Collins, *J. Struct. Geol.* **20**, 1273 (1998).
28. A. F. Glazner, J. M. Bartley, D. S. Coleman, W. Gray, R. Z. Taylor, *GSA Today* **14**, 4 (2004).
29. C. Annen, J. D. Blundy, R. S. J. Sparks, *J. Petrol.* **47**, 505 (2005).
30. M. D. Jackson, M. J. Cheadle, M. P. Atherton, *J. Geophys. Res.* **108**, 2332 (2003).
31. S. Couch, R. S. J. Sparks, M. R. Carroll, *Nature* **411**, 1037 (2001).
32. C. J. Hawkesworth, A. I. S. Kemp, *Nature* **443**, 811 (2006).
33. J. R. O. Neil, B. W. Chappell, *J. Geol. Soc. London* **133**, 559 (1977).

34. We are indebted to J. Craven for guidance with oxygen isotope analysis at the Edinburgh Ion Microprobe Facility and to C. Coath for assistance with Hf isotope analysis at Bristol. R. Arculus, N. Pearson, and C. Graham generously provided advice at the outset of the study. Constructive comments by S. Sparks, B. Collins, and two reviewers are gratefully acknowledged. Funded by NERC grants NER/I/S/00942 and IMP/250/505.

Supporting Online Material

www.sciencemag.org/cgi/content/full/315/5814/980/DC1
Materials and Methods
SOM Text
Tables S1 to S5
References

11 October 2006; accepted 11 January 2007
10.1126/science.1136154

Fracture-Controlled Paleo-Fluid Flow in Candor Chasma, Mars

Chris H. Okubo* and Alfred S. McEwen

Color observations from the High Resolution Imaging Science Experiment on board the Mars Reconnaissance Orbiter reveal zones of localized fluid alteration (cementation and bleaching) along joints within layered deposits in western Candor Chasma, Mars. This fluid alteration occurred within the subsurface in the geologic past and has been exposed at the surface through subsequent erosion. These findings demonstrate that fluid flow along fractures was a mechanism by which subsurface fluids migrated through these layered deposits. Fractured layered deposits are thus promising sites for investigating the geologic history of water on Mars.

The High Resolution Imaging Science Experiment (HiRISE) camera (*1*, *2*) on board the Mars Reconnaissance Orbiter (MRO) has returned images of the surface of Mars that have exceptional clarity and resolution. One of the first images of Mars returned by HiRISE in the low (250 to 315 km) mapping orbit is of the layered deposits within western Candor Chasma (Fig. 1 and fig. S1), one of the larger canyons of the Valles Marineris system, in the western equatorial region of Mars (fig. S2). Surface features $\gtrsim$0.26 m (equivalent to one pixel) are detectable, and the shapes of objects $\gtrsim$0.78 m across are resolved (*2*).

The layered deposits appear as alternating light- and dark-toned bands (Fig. 1 and fig. S1) and may be volcanic, eolian, or lacustrine in origin (*3*–*6*). The dark bands appear to be flat-lying in many areas at the 10-m scale. Many of the dark-toned bands consist of a mixture of meter-scale boulders of light-toned material and finer-grained dark material (figs. S3 and S4). The patches of fine-grained dark material commonly have a hummocky texture that is consistent with ripples of ~2 to 5 m in wavelength (fig. S3). Evidence of recent eolian activity is pervasive throughout the scene [supporting online material (SOM) text]. Therefore, this flat-lying dark material is interpreted as surficial deposits of sediment composed of eolian sand, with a possible component of lag. Dark material within the underlying bedrock may also contribute to the tone of the dark bands.

The source of the dark-toned sediment is unconstrained by the present study, but it may be present within the underlying bedrock and became mobilized through eolian erosion or persists in place as lag deposits. Dark material may also have been transported from a distal source.

Local topography and high surface roughness of select layers within the light-toned bedrock apparently contribute to the accumulation of the dark sediment in distinct bands (figs. S3 to S5). The dark-toned bands are commonly found within topographic depressions in the underlying bedrock. Accumulations of boulders also act to trap dark-toned sediment within the bands (SOM text). Thus, the dark-toned bands appear to consist of sediment that has accumulated within the troughs between ridges of light-toned bedrock.

This ridge-and-trough morphology is consistent with differential erosion, which can be

---

Lunar and Planetary Laboratory, University of Arizona, Tucson, AZ 85721, USA.

*To whom correspondence should be addressed. E-mail: chriso@lpl.arizona.edu

expected if the bedrock is mechanically layered. That is, the mechanically weaker layers of rock have faster erosion rates than the stronger layers. Assuming a homogeneous digenetic history, fine-grained layers are stronger than coarse-grained layers within the same sedimentary deposit (*7*). The coarser-grained layers erode faster than the finer-grained layers, resulting in a ridge-and-trough morphology as suggested here. Local heterogeneities in cementation and chemical weathering may also influence rock strength (*8*–*10*). Thus, the ridges and troughs within the bedrock may reflect local variations in either grain size or diagenetic history, or both.

Also present are sets of fractures that are hundreds of meters to several kilometers in length (Figs. 1 and 2 and fig. S3). Shear displacements of crosscut bedding and other discontinuities are not observed along these fractures. Small horizontal displacements of more than 0.52 m (two pixels) would be clearly observed at the resolution of the HiRISE image. Therefore, these fractures are identified as joints rather than faults (SOM text).

Many joints are surrounded by a nearly continuous "halo" of light-toned bedrock that cuts across the dark-toned bands (Fig. 2 and figs. S3 and S4). These joint halos are interrupting the background pattern of sediment patches, or topographic depressions, and any layers of bedrock that are dark. The lack of dark material points to a negligible accumulation of dark sediment along these halos, as well as a systematic lightening of any dark layers of bedrock within these halos.

The negligible amount of dark material along the joint halos indicates that these areas are unfavorable for sediment deposition. A lack of meter-scale topographic shading along the bedrock within the halos reveals that these surfaces are smooth at the meter scale. In contrast, the adjacent light-toned bands show clear topographic shading that is distinguishable from albedo variations through HiRISE's color capability (Fig. 2 and figs. S3 and S4). The surface along the joint halos is therefore interpreted to be smoother at the meter scale relative to the adjacent light- and dark-toned bands. A smoother ground surface means a lack of small-scale topography that can act to trap sediment.

Patterns of topographic shading also indicate that the joint halos often have a positive relief with inclined surfaces that would tend to impede sediment accumulation. By analogy with the light-toned bands, the accumulation of dark sediment along the trace of the joint can be inhibited where the halos are ridgelike. A ridgelike morphology for the joint halos requires the bedrock along the joints to have been strengthened against erosion. Ridgelike segments of the halos that crosscut the dark-toned bands of sediment especially need to be strengthened because, presumably, these dark bands lie along mechanically weaker (more-eroded) layers of bedrock.

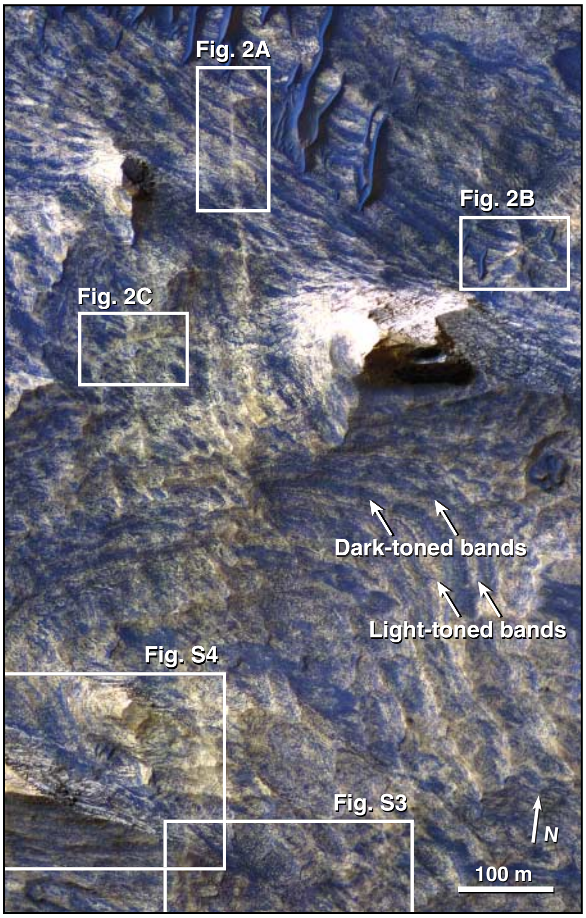

Fig. 1. High-resolution enhanced-color image showing a landscape of sand dunes and buttes against a background of light-toned (tan) and dark-toned (blue) bands in Candor Chasma. This is a subscene from HiRISE image TRA_000836_1740, which was acquired on 30 September 2006 (Mars southern winter). The image was taken at the local Mars time of 3:29 p.m., and the scene was illuminated from the west with a solar incidence angle of 58.5°. The HiRISE camera collected image data in three band passes (blue-green, red, and near-infrared; 400 to 1000 nm) (*1*, *2*). The image scale is 0.26 m per pixel, which is equivalent to the scale of the red band-pass image. The other band passes were acquired with two-by-two pixel binning to 0.52 m per pixel. The complete image is centered at –5.7° latitude, 284.6°E longitude (planetocentric, International Astronomical Union 2000).

The combination of a smooth surface and positive relief along the joint halos accounts for the lack of accumulated dark sediment and indicates that the bedrock within these halos is stronger (more indurated) than the more readily eroded bedrock around it. Chemical precipitation of minerals (e.g., Fe-bearing minerals) (*11*–*13*) from fluids circulating within pore spaces of the rock along the haloed joints is a likely mechanism of wall-rock strengthening. These minerals act to cement the wall rock and thereby increase the rock's resistance to pitting and erosion.

These halos most plausibly formed after the joints were present. Had the halos formed first as nonfractured mechanically strong ridges, the joints would have preferentially propagated within the weaker rock adjacent to those halos, rather than through the center of the halos as is observed. Preexisting joints would also facilitate the localization of bleaching and cementation within distinct linear halos by acting as conduits for circulating fluids. In the absence of fracture-controlled fluid flow, diagenetic alteration would be distributed throughout the rock mass rather than being localized in discrete zones that crosscut bedding (e.g., *11*–*16*).

The systematic lightening in tone of any dark bedrock layers along the halos points to geochemical bleaching of the bedrock. As previously mentioned, dark material may contribute to the appearance of the dark-toned bands, especially on slopes. However, dark bedrock is lacking within the joint halos. Thus, any dark material originally present within the bedrock appears to have been dissolved or geochemically altered within the halos.

On Earth, the bleaching of the rock surrounding a fracture is a clear indication of chemical interactions between the fluids circulating within that fracture and the host rock (*11*, *12*). Additionally, interactions between the wall rock and the fluids flowing through the fracture induce changes in the strength of the wall rock (*8*–*10*). Fracture-supported flow is recognized as an important process that facilitates the large-scale subsurface migration of fluids and chemical interactions between these fluids and the host rock (*8*, *9*, *15*, *16*).

The strengthening of the joints' wall rock, as well as the geochemical bleaching of this rock, provides strong evidence of subsurface fluids having circulated through this section of the layered deposits. These episodes of bleaching and cementation probably reflect episodes of reducing and oxidizing fluid flow, as is commonly observed on Earth (*11–13*) and also on Mars (*17–19*). These results support previous findings from the Observatoire pour la Minéralogie, l'Eau, les Glaces, et l'Activité (OMEGA) hyperspectral imager on board Mars Express. OMEGA observations of this region of the layered deposits reveal the spectral signature of hydrated sulfates, which is viewed as evidence of past aqueous activity (*20*, *21*).

Not all joints in this scene have halos (fig. S5). This is probably because of a difference in age for the haloed versus "non-haloed" joints. Halos developed around joints that were present when subsurface fluids were circulating through the currently exposed level of the bedrock. Once the bulk of the subsurface fluids drained from this area, any new joints that formed would not have supported adequate fluid flow for a sufficient amount of time to allow for the strengthening and bleaching of the wall rock to occur; thus, no halo is present. Therefore, the presence of halos may be a proxy for relative fracture age, with the haloed fractures being the oldest and the non-haloed fractures being the youngest and having formed after the subsurface fluids drained from this level of the bedrock.

The presence of non-haloed joints that apparently postdate the haloed joints indicates that halo formation, and thus circulation of subsurface fluids within these joints, was not a geologically recent event. Further, had the haloed joints supported geologically recent near-surface fluid flow, fluvial erosional and depositional structures would be apparent (*22, 23*). Such morphologic evidence for recent subaerial fluid flow (e.g., gullies and spring mounds) is not observed. Thus, the present-day exposures of the haloed joints initially formed within the subsurface as fluids circulated through the layered deposits. These fluids subsequently drained away, and the haloed joints were exposed at the surface through erosion. Therefore, evidence of geochemical processes that once occurred within the subsurface is currently exposed at the surface in the form of these haloed joints.

A current focus of Mars surface exploration is the investigation of areas that show evidence of past hydrologic activity, with the intent of characterizing the past habitability of these areas and their potential to support life. Much attention has been paid to classic volatile-related terrains such as dry river- and lakebeds and paleo-springs. This study demonstrates that exhumed joints and faults are also promising areas in which to investigate past hydrologic activity. In addition to Fig. 1, haloed joints are observed in other HiRISE images of equatorial layered deposits in Valles Marineris and elsewhere. Further analyses of these fractures may yield additional insight into the geochemistry that drives the bleaching and cementation of the wall rock.

Detailed surface observations of fracture-controlled fluid flow may be possible with the Mars Exploration Rover Opportunity. A separate HiRISE image of Victoria Crater in Meridiani Planum reveals a set of subparallel linear ridges along the crater's eastern rim and floor (fig. S6). These ridges are stratigraphically located within the regional layered sedimentary bedrock. The linearity, common orientation, and positive relief of these features suggest that these are fractures that are surrounded by bedrock that has been chemically cemented or otherwise indurated, similar to the joints described here in Candor Chasma. Opportunity is currently at Victoria Crater, and detailed studies of these ridges may provide additional insight into the mechanics and chemistry of paleo-fluid flow through the regional sedimentary bedrock.

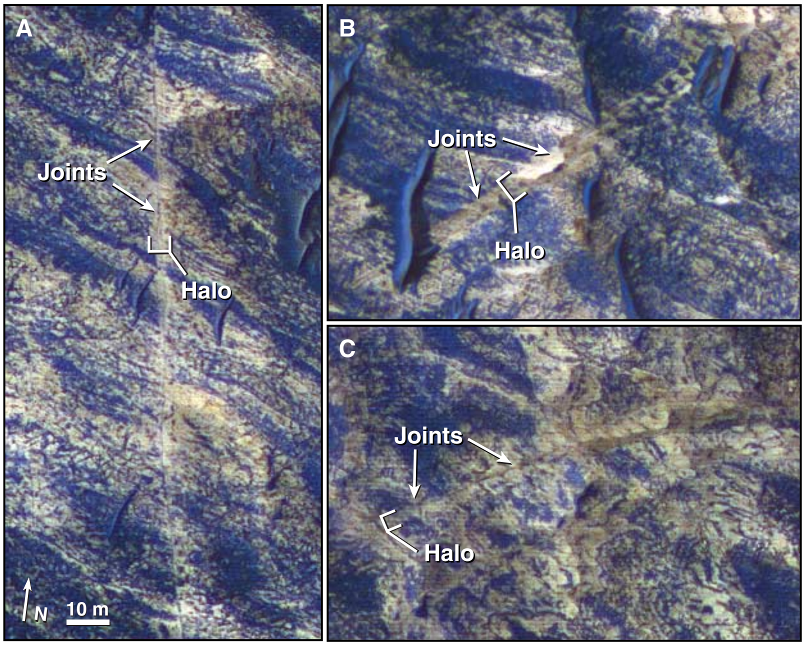

Fig. 2. (**A** to **C**) Examples of joints and surrounding halos of light-toned bedrock. The joints are the thin dark lineations. The scale bar and north arrow apply to each panel.

References and Notes

1. A. S. McEwen *et al.*, *J. Geophys. Res.*, in press.
2. For more information on HiRISE, see http://hirise.lpl.arizona.edu.
3. N. E. Witbeck, K. L. Tanaka, D. H. Scott, *Geologic Map of the Valles Marineris Region of Mars*, scale 1:2,000,000, *U.S. Geol. Surv. Misc. Geol. Invest. Map I-2010* (U.S. Geological Survey, Denver, CO, 1991).
4. B. K. Lucchitta *et al.*, *Mars* (Univ. of Arizona Press, Tucson, AZ, 1992), pp. 423–492.
5. S. Murchie, L. Kirkland, S. Erard, J. Mustard, M. Robinson, *Icarus* **147**, 444 (2000).
6. M. G. Chapman, K. L. Tanaka, *Icarus* **155**, 324 (2002).
7. T.-f. Wong, C. David, W. Zhu, *J. Geophys. Res.* **102**, 3009 (1997).
8. K. J. W. McCaffrey, L. Lonergan, J. J. Wilkinson, *Fractures, Fluid Flow and Mineralization* (Special Publication 155, Geological Society of London, London, 1999).
9. B. Jamtveit, B. Yardley, *Fluid Flow and Transport in Rocks* (Chapman & Hall, London, 1997).
10. National Research Council, *Rock Fractures and Fluid Flow: Contemporary Understanding and Applications* (National Academy Press, Washington, DC, 1996).
11. M. A. Chan, B. B. Bowen, W. T. Parry, J. Ormö, G. Komatsu, *Geol. Soc. Am. Today* **15** (no. 8), 4 (2005).
12. M. A. Chan, W. T. Parry, J. R. Bowman, *Am. Assoc. Pet. Geol. Bull.* **84**, 1281 (2000).
13. M. A. Chan, B. Beitler, W. T. Parry, J. Ormö, G. Komatsu, *Nature* **429**, 731 (2004).
14. B. Beitler, W. T. Parry, M. A. Chan, *J. Sediment. Res.* **75**, 547 (2005).
15. W. T. Parry, M. A. Chan, B. Beitler, *Am. Assoc. Pet. Geol. Bull.* **88**, 175 (2004).
16. B. Beitler, M. A. Chan, W. T. Parry, *Geology* **31**, 1041 (2003).
17. B. C. Clark *et al.*, *Earth Planet. Sci. Lett.* **240**, 73 (2005).
18. S. M. McLennan *et al.*, *Earth Planet. Sci. Lett.* **240**, 95 (2005).
19. N. J. Tosca *et al.*, *Earth Planet. Sci. Lett.* **240**, 122 (2005).
20. J.-P. Bibring *et al.*, *Science* **312**, 400 (2006).
21. A. Gendrin *et al.*, *Science* **307**, 1587 (2005).
22. Z. K. Shipton *et al.*, *Geological Storage of Carbon Dioxide* (Geological Society of London, London, 2004), pp. 43–58.
23. M. C. Malin, K. S. Edgett, L. V. Posiolova, S. M. McColley, E. Z. Noe Dobrea, *Science* **314**, 1573 (2006).

24. We are grateful to the science, operations, and engineering teams of HiRISE and the MRO project, whose diligent efforts made this work possible. Comments by HiRISE team members and two anonymous reviewers are also appreciated. Portions of this work were conducted under contract with NASA, with additional support by a grant from NASA's Mars Data Analysis Program.

Supporting Online Material

www.sciencemag.org/cgi/content/full/315/5814/983/DC1
SOM Text
Figs. S1 to S6
References

27 October 2006; accepted 19 December 2006
10.1126/science.1136855